Science Advances
AAAS

Supplementary Materials for

Microsecond dynamics control the HIV-1 Envelope conformation

Ashley L. Bennett *et al.*

Corresponding author: Rory Henderson, rory.henderson@duke.edu

Sci. Adv. **10**, eadj0396 (2024)
DOI: 10.1126/sciadv.adj0396

This PDF file includes:

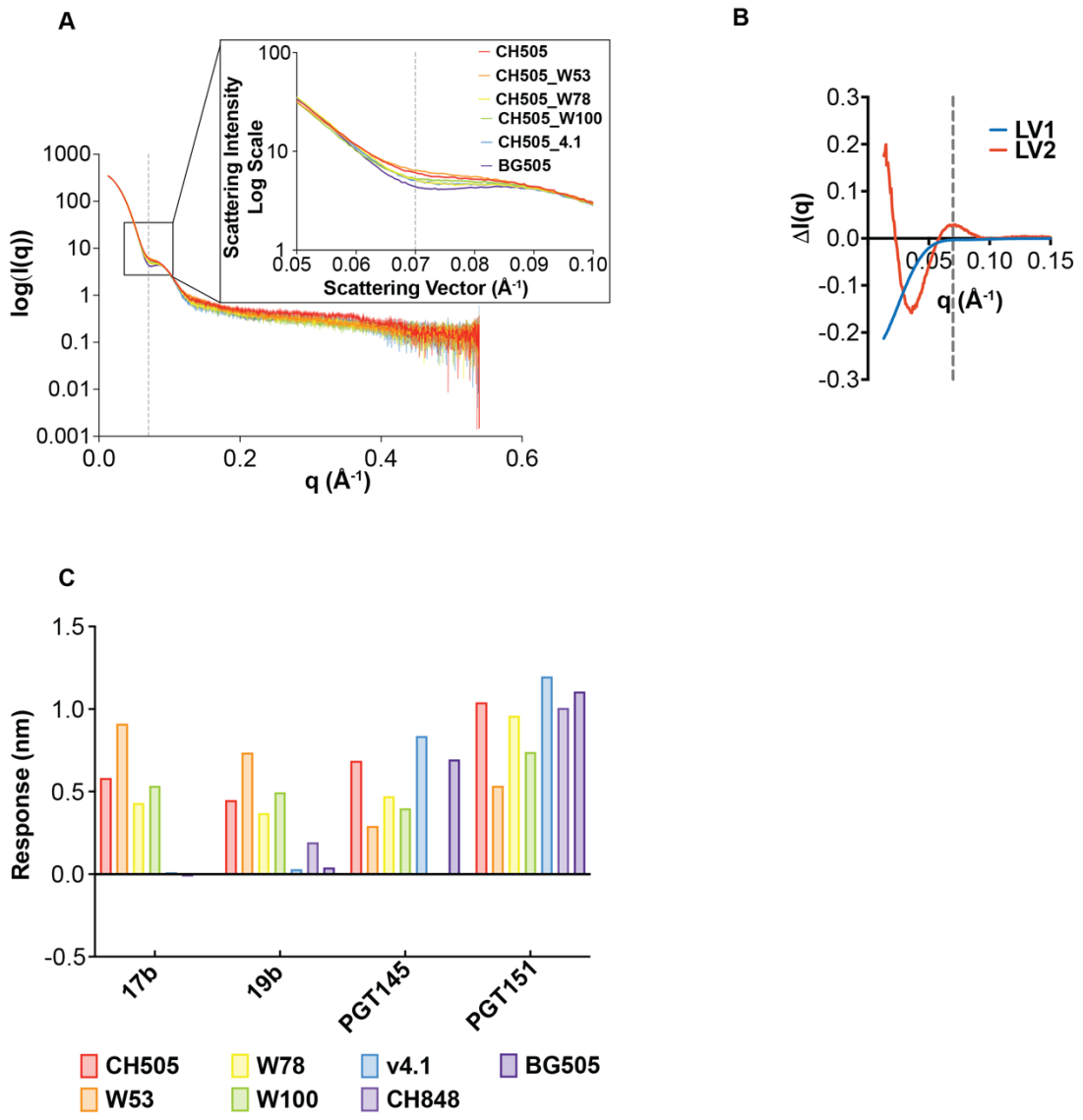

Supplemental Figure 1: SAXS profiles reflect the degree of Env SOSIP opening. (A) Static SAXS profiles for CH505 (*red*), CH505 week 53 (*orange*), CH505 week 78 (*yellow*), CH505 week 100 (*green*), CH505 v4.1 (*blue*), and BG505 (*violet*). The scattering intensity is expressed on the y-axis as a function of the scattering vector in $Å^{-1}$. The box shows the region of the scattering profile displayed in the inset. The grey dashed line indicates the feature peak at q = 0.07$Å^{-1}$. **(B)** The SVD left vector 1 (*blue*) and left vector 2 (*red*) on the CH505 and BG505 SOSIP panel. The grey dashed line indicates the feature of interest at q = 0.07$Å^{-1}$. (C) BLI binding response for CH505 (*red*) CH505 week 53 (*orange*), CH505 week 78 (*yellow*), CH505 week 100 (*green*), CH505 v4.1 (*blue*), CH848 (*lavender*), and BG505 (*violet*).

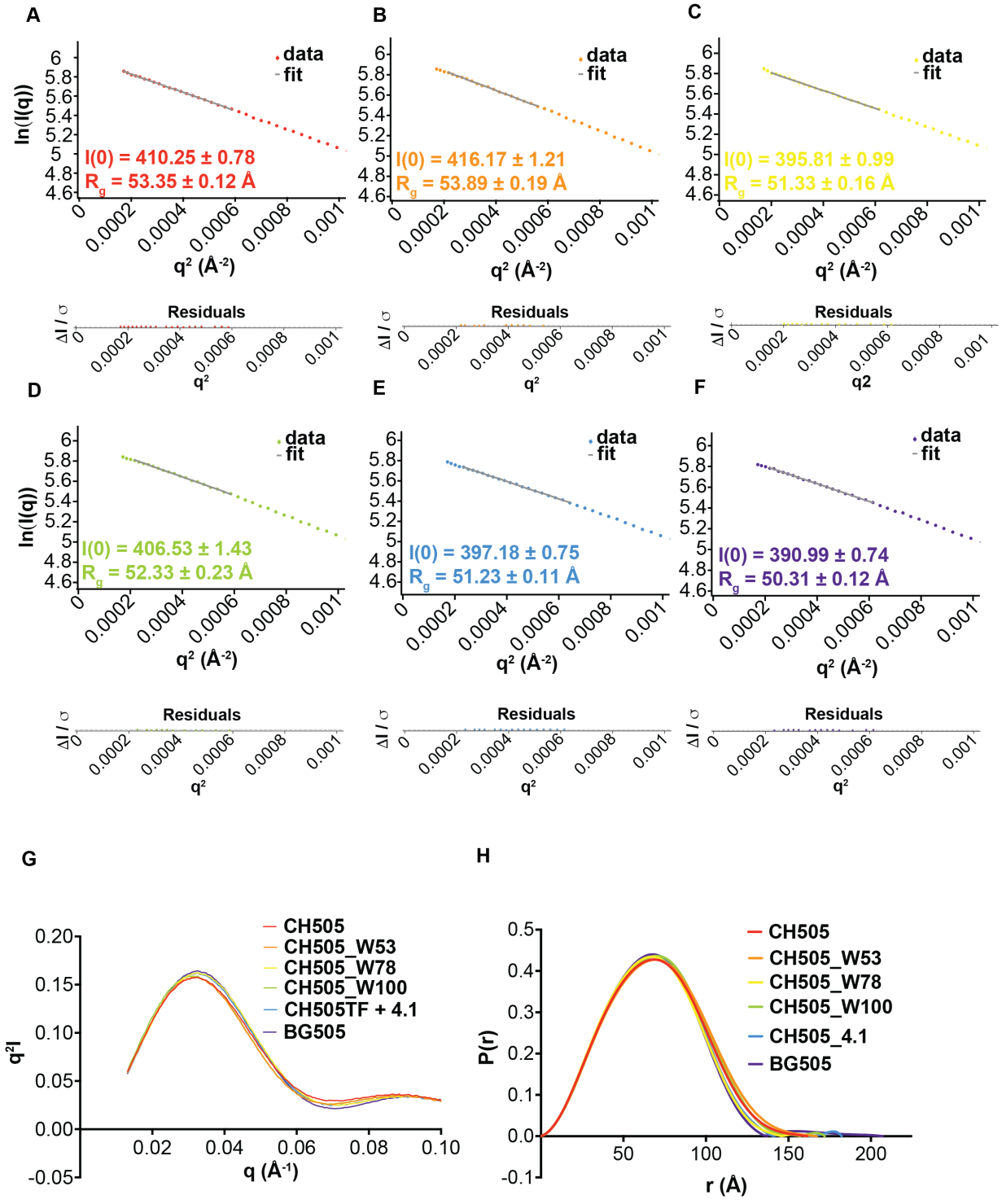
A
B
C
D
E
F
G
H
ln(I(q))
data
fit
I(0) = 410.25 ± 0.78
Rg = 53.35 ± 0.12 Å
I(0) = 416.17 ± 1.21
Rg = 53.89 ± 0.19 Å
I(0) = 395.81 ± 0.99
Rg = 51.33 ± 0.16 Å
I(0) = 406.53 ± 1.43
Rg = 52.33 ± 0.23 Å
I(0) = 397.18 ± 0.75
Rg = 51.23 ± 0.11 Å
I(0) = 390.99 ± 0.74
Rg = 50.31 ± 0.12 Å
q² (Å⁻²)
Residuals
ΔI / σ
q²
q2
q²I
q (Å⁻¹)
P(r)
r (Å)
CH505
CH505_W53
CH505_W78
CH505_W100
CH505TF + 4.1
CH505_4.1
BG505

Supplemental Figure 2: Env SOSIPs are stable under static SAXS conditions. The Guinier analysis of **(A)** CH505 (*red*), **(B)** CH505 week 53 (*orange*), **(C)** CH505 week 78 (*yellow*), **(D)** CH505 week 100 (*green*), **(E)** CH505 v4.1 (*blue*), and **(F)** BG505 (*purple*) Env SOSIP SAXS profiles at 35°C. **(G)** Kratky plots for CH505 (*red*), CH505 week 53 (*orange*), CH505 week 78 (*yellow*), CH505 week 100 (*green*), CH505 v4.1 (*blue*), and BG505 (*violet*). **(H)** The pair distance distribution (P(r)) for CH505 (*red*), CH505 week 53 (*orange*), CH505 week 78 (*yellow*), CH505 week 100 (*green*), CH505 v4.1 (*blue*), and BG505 (*violet*).

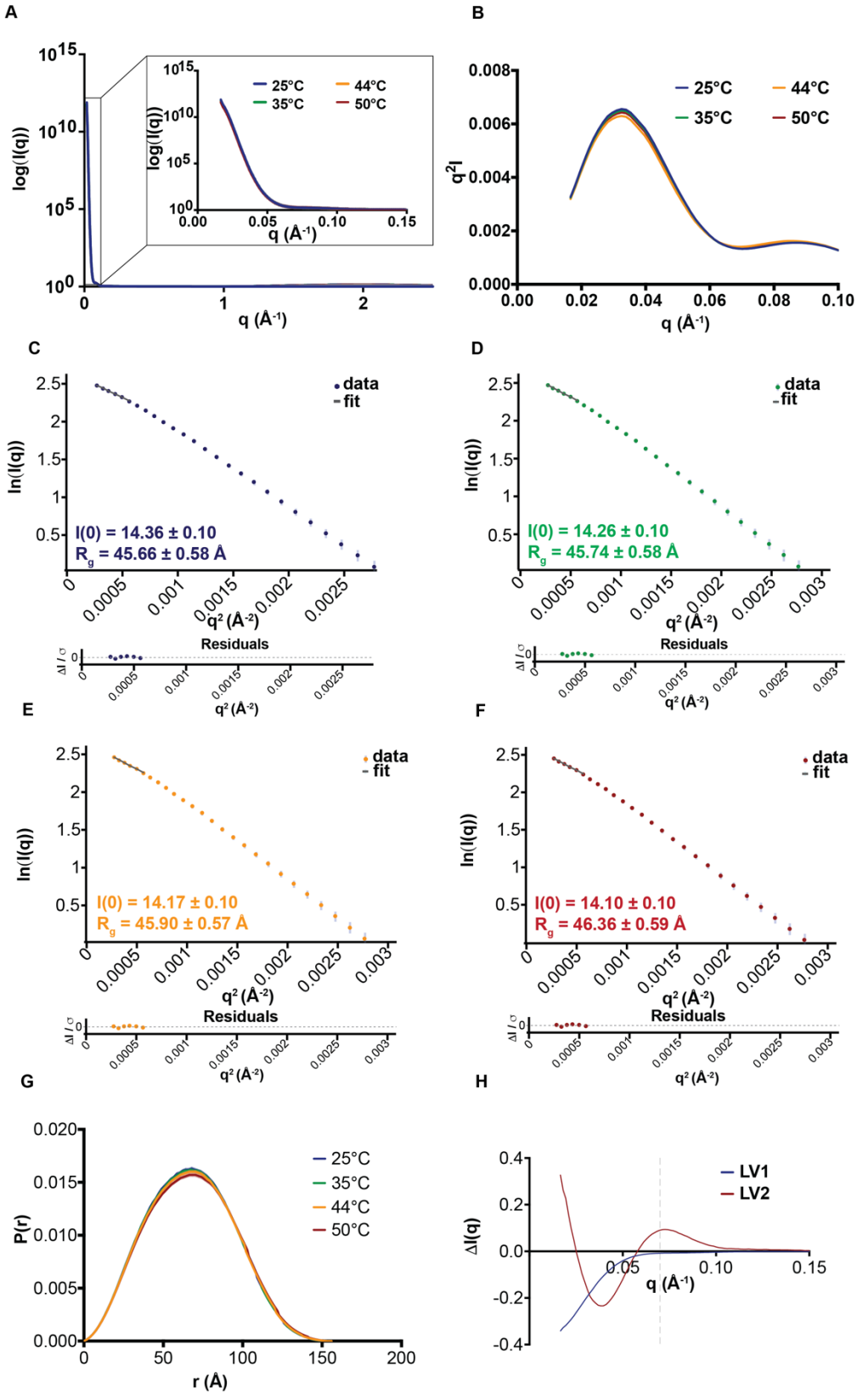
A
log(I(q))
q (Å-1)
25°C
35°C
44°C
50°C
B
q2I
q (Å-1)
C
ln(I(q))
data
fit
I(0) = 14.36 ± 0.10
Rg = 45.66 ± 0.58 Å
Residuals
q2 (Å-2)
D
I(0) = 14.26 ± 0.10
Rg = 45.74 ± 0.58 Å
E
I(0) = 14.17 ± 0.10
Rg = 45.90 ± 0.57 Å
F
I(0) = 14.10 ± 0.10
Rg = 46.36 ± 0.59 Å
G
P(r)
r (Å)
H
ΔI(q)
LV1
LV2

Supplemental Figure 3: CH505 HIV-1 Env SOSIP is stable under SAXS at elevated temperatures. (A) Static SAXS profiles for CH505 Env SOSIP at 25°C (blue), 35°C (green), 44°C (yellow), and 50°C (red). The scattering intensity is expressed on the y-axis as a function of the scattering vector in $Å^{-1}$. The box shows the region of the scattering profile displayed in the inset. **(B)** The Kratky plots for CH505 SOSIP at 25°C (blue), 35°C (green), 44°C (yellow), and 50°C (red). **(C)** Guinier analysis of CH505 Env SOSIP SAXS profiles at 25°C. **(D)** The Guinier analysis of CH505 Env SOSIP SAXS profiles at 35°C. **(E)** The Guinier analysis of CH505 Env SOSIP SAXS profiles at 44°C. **(F)** The Guinier analysis of CH505 Env SOSIP SAXS profiles at 50°C. **(G)** The pair distance distribution (P(r)) for CH505 Env SOSIP at 25°C, 35°C, 44°C, and 50°C in blue, green, yellow, and red, respectively. **(H)** SVD left vector 1 (*blue*) and SVD left vector 2 (*red*) on the CH505 static SAXS scattering curves.

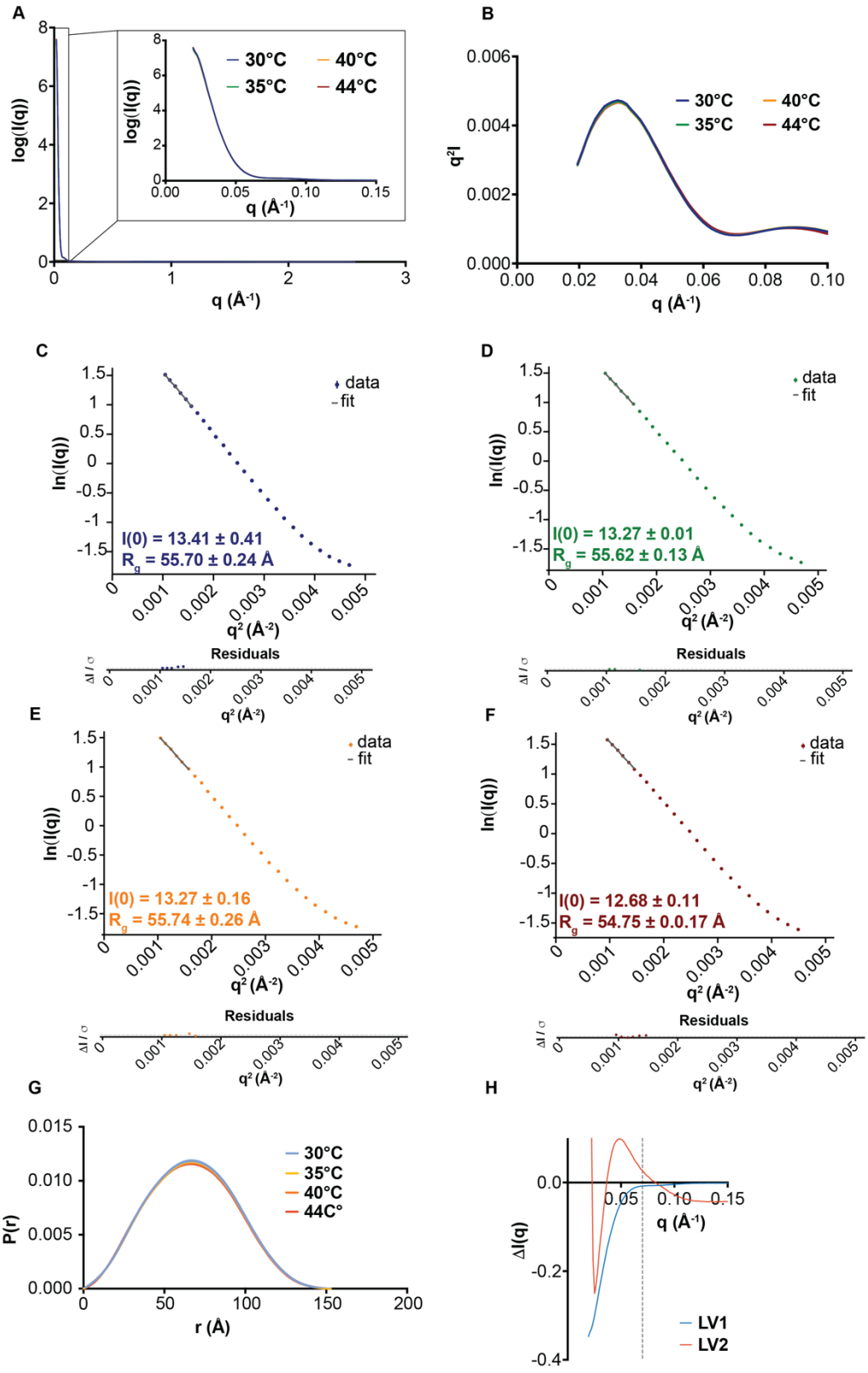
A
log(I(q))
q (Å-1)
30°C
35°C
40°C
44°C
B
q²I
q (Å-1)
C
ln(I(q))
data
fit
I(0) = 13.41 ± 0.41
Rg = 55.70 ± 0.24 Å
q² (Å-2)
Residuals
ΔI / σ
D
I(0) = 13.27 ± 0.01
Rg = 55.62 ± 0.13 Å
E
I(0) = 13.27 ± 0.16
Rg = 55.74 ± 0.26 Å
F
I(0) = 12.68 ± 0.11
Rg = 54.75 ± 0.0.17 Å
G
P(r)
r (Å)
H
ΔI(q)
LV1
LV2

Supplemental Figure 4: CH848 Env SOSIP is stable under SAXS at elevated temperatures. (A) Static SAXS profiles for CH848 Env SOSIP at 30°C (*blue*), 35°C (*green*), 40°C (*yellow*), and 44°C (*red*). The scattering intensity is expressed on the y-axis as a function of the scattering vector in $Å^{-1}$. The box shows the region of the scattering profile displayed in the inset. **(B)** The Kratky plots for CH848 SOSIP at 30°C (*blue*), 35°C (*green*), 40°C (*yellow*), and 44°C (*red*). **(C)** Guinier analysis of CH848 Env SOSIP SAXS profiles at 30°C. **(D)** The Guinier analysis of CH848 Env SOSIP SAXS profiles at 35°C. **(E)** The Guinier analysis of CH848 Env SOSIP SAXS profiles at 40°C. **(F)** The Guinier analysis of CH848 Env SOSIP SAXS profiles at 44°C. **(G)** The pair distance distribution (P(r)) for CH848 Env SOSIP at 30°C, 35°C, 40°C, and 44°C in blue, green, yellow, and red, respectively. **(H)** SVD left vector 1 (*blue*) and SVD left vector 2 (*red*) on the CH848 static SAXS scattering curves.

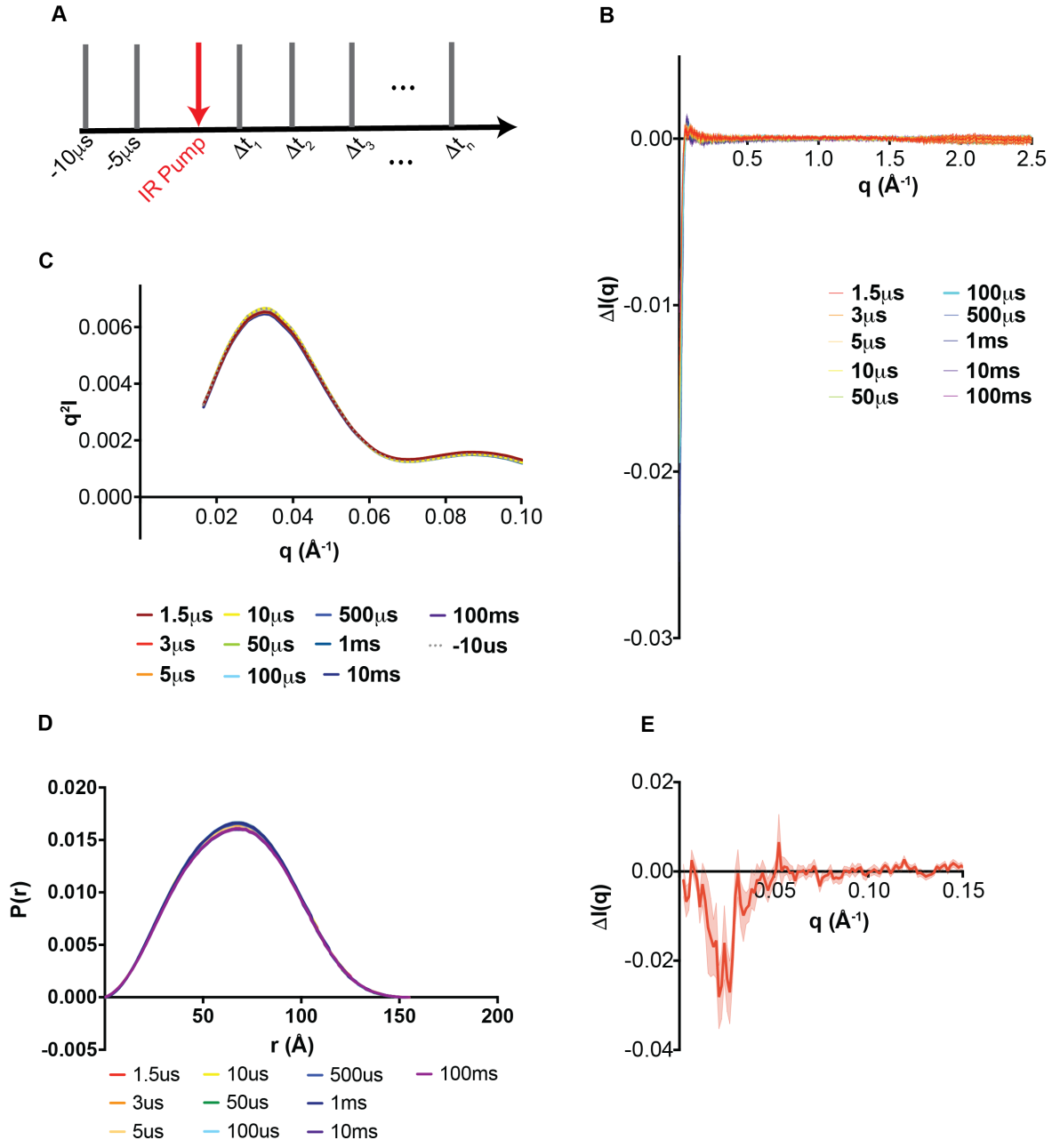

Supplemental Figure 5: CH505 Env SOSIP shows time-dependent changes in SAXS profiles. (A) Experimental protocol for the pump-probe set up. The horizontal black arrow represents the progression of time during the experiment. The grey bars represent the X-ray probe step, and the red bars represent the infrared laser pump step. For the time resolved (TR) temperature-jump (T-jump) SAXS experiments, the X-ray scattering was collected at 2 time points (-10μs and -5μs) prior to the infrared laser pump and then the IR pump step is interleaved with the X-ray probe at various time delays after the IR pump. The time delays measured for this experiment range from 1.5μs to 100ms as well as 500ns **(B)** TR, T-Jump SAXS scattering difference curves for 1.5μs (*red*), 3μs (*orange*), 5μs (*light orange*), 10μs (*yellow*), 50μs (*green*), 100μs (*cyan*), 500μs (*blue*), 1ms (*indigo*), 10ms (*violet*), and 100ms (*magenta*) time delays.

Shaded regions represent the standard error of the arithmetic mean. **(C)** The Kratky plots for CH505TF Env SOSIP at 1.5μs (red), 3μs (orange), 5μs (light orange), 10μs (yellow), 50μs (green), 100μs (cyan), 500μs (blue), 1ms (indigo), 10ms (violet), and 100ms (magenta) time delays. **(D)** The pair distance distributions for CH505 Env SOSIP at 1.5μs (*red*), 3μs (*orange*), 5μs (*light orange*), 10μs (*yellow*), 50μs (*green*), 100μs (*cyan*), 500μs (*blue*), 1ms (*indigo*), 10ms (*violet*), and 100ms (*magenta*) time delays. **(E)** TR, T-Jump SAXS scattering difference curves for 500ns with the change in scattering intensity are plotted as a function of the scattering vector in $Å^{-1}$. The shaded areas represent the standard error of the arithmetic mean.

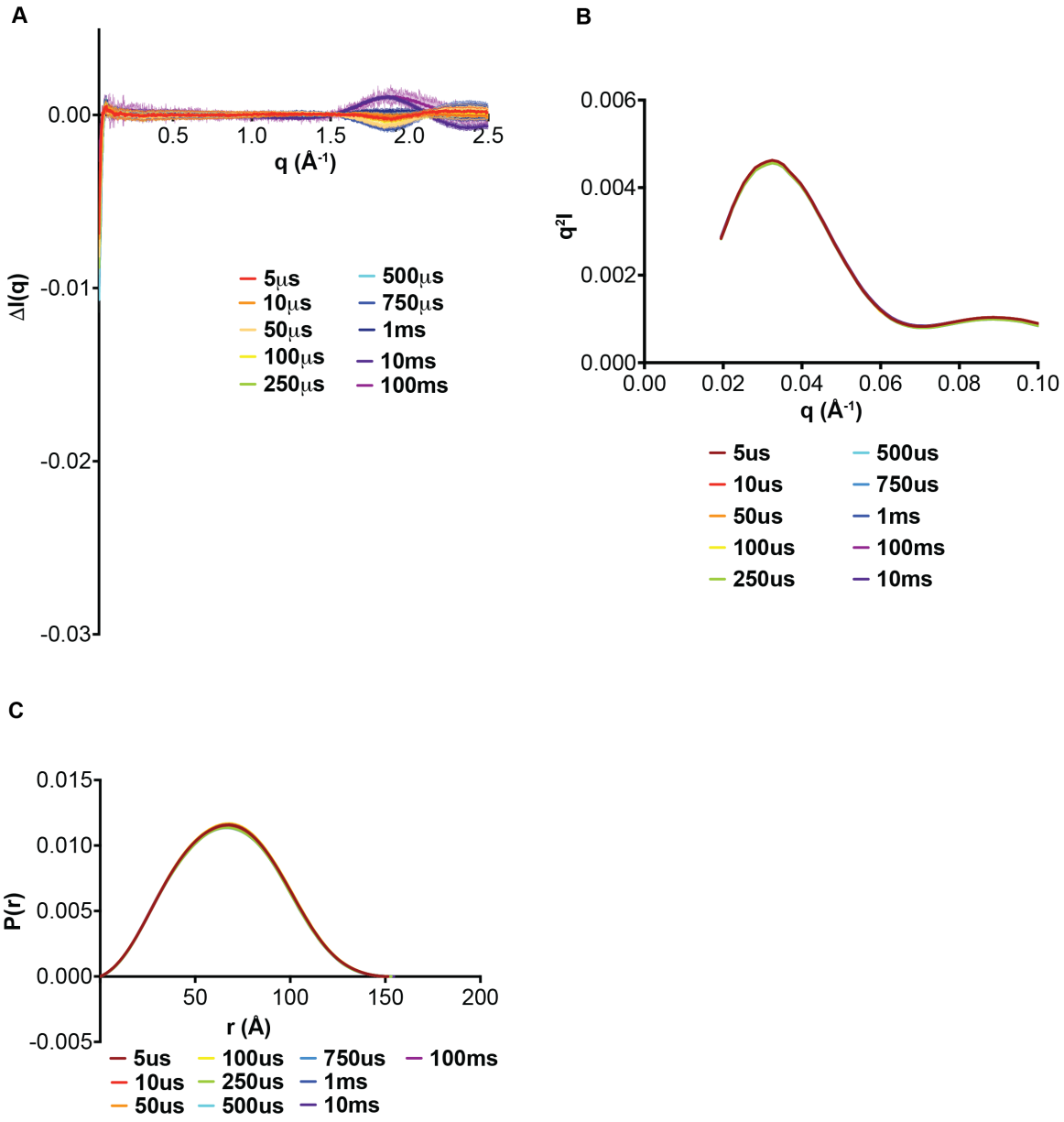

Supplemental Figure 6: CH848 Env SOSIP shows time-dependent changes in SAXS profiles. (A) TR, T-Jump SAXS scattering difference curves for 5μs (*red*), 10μs (*orange*), 50μs (*light orange)*, 100μs (*yellow*), 250μs (*green*), 500μs (*cyan*), 750μs (*blue*), 1ms (*indigo*), 10ms

(*violet*), and 100ms (*magenta*) time delays. Shaded regions represent the standard error of the arithmetic mean. **(B)** The Kratky plots for CH848 Env SOSIP at 5μs (*red*), 5μs (*orange*), 50μs (*light orange*), 100μs (*yellow*), 250μs (*green*), 500μs (*cyan*), 750μs (*blue*), 1ms (*indigo*), 10ms (*violet*), and 100ms (*magenta*) time delays. **(C)** The pair distance distributions for CH848 Env SOSIP at 5μs (*red*), 10μs (*orange*), 50μs (*light orange)*, 100μs (*yellow*), 250μs (*green*), 500μs (*cyan*), 750μs (*blue*), 1ms (*indigo*), 10ms (*violet*), and 100ms (*magenta*) time delays.

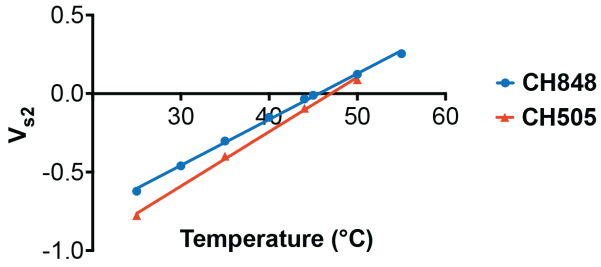

Supplemental Figure 7: Calibration of TR, T-Jump. Linear fit of the second right vectors of SVD on the pooled T-Jump and static SAXS profiles for CH505 (*red*) and CH848 (*blue*).

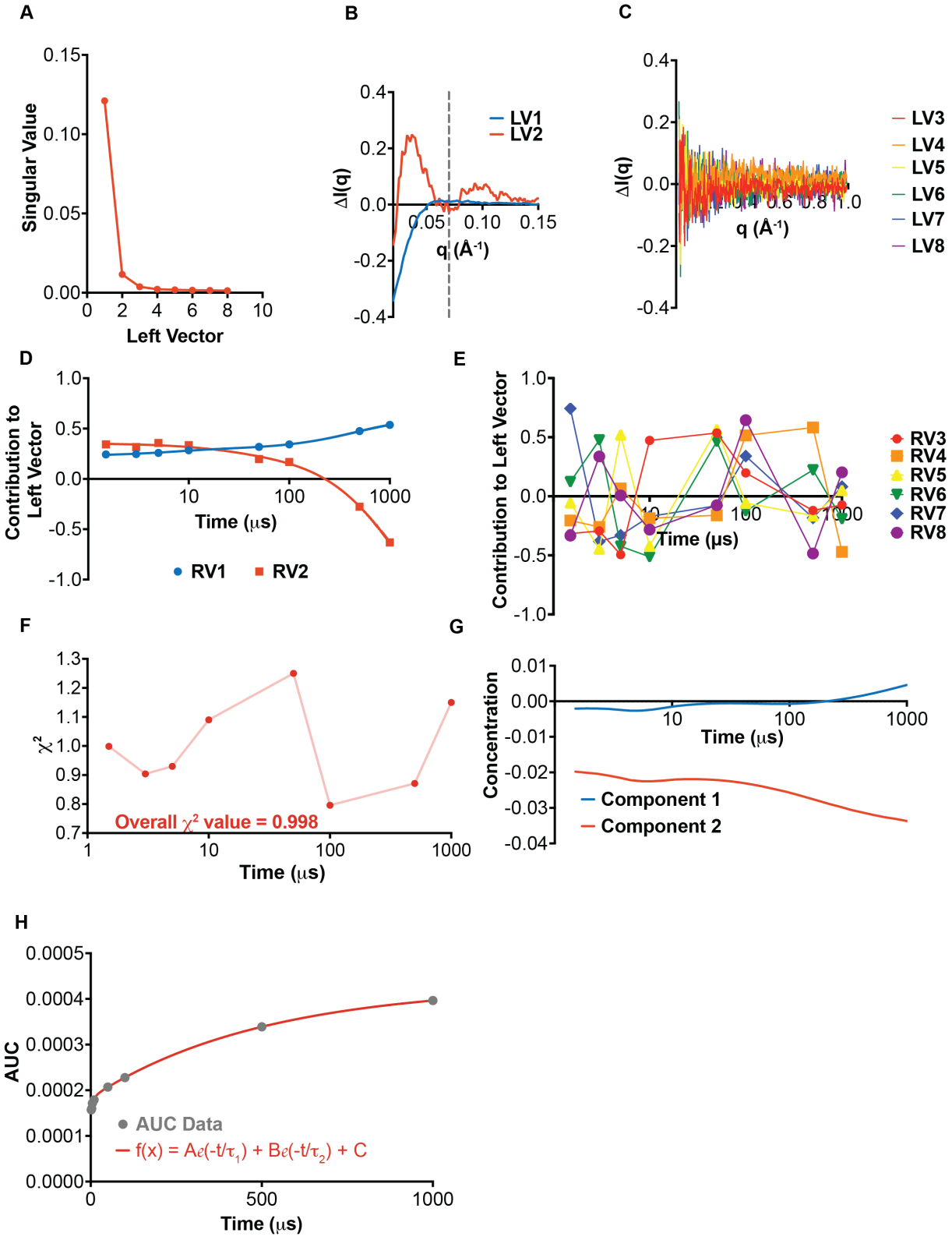

Supplemental Figure 8: Decomposition of CH505 Env SOSIP TR, T-Jump SAXS Difference Profiles. (A) The singular values of SVD on CH505 Env SOSIP TR, T-Jump difference profiles

plotted as a function of the extracted SVD vector. **(B)** Singular value decomposition left vectors 1 (*LV1, blue*) and 2 (*LV2, red*). The dashed grey line at q=0.07Å^{-1} indicates the location of the feature peak. **(C)** CH505 Env SOSIP TR, T-Jump SVD left vectors 3-8. **(D)** Double exponential fits to the SVD right vectors 1 (*RV1, blue*) and 2 (*RV2, red*) showing the contribution of LV1 and LV2 at each time delay. **(E)** CH505 Env SOSIP TR, T-Jump SVD right vectors 3-8. **(F)** c^2 values of the REGALS fit to the TR, T-Jump SAXS data. **(G)** The REGALS concentrations extracted for REGALS component 1 (*blue*) and component 1 (*red*). **(H)** Double exponential fit to AUC for CH505 TR, T-Jump SAXS difference curves.

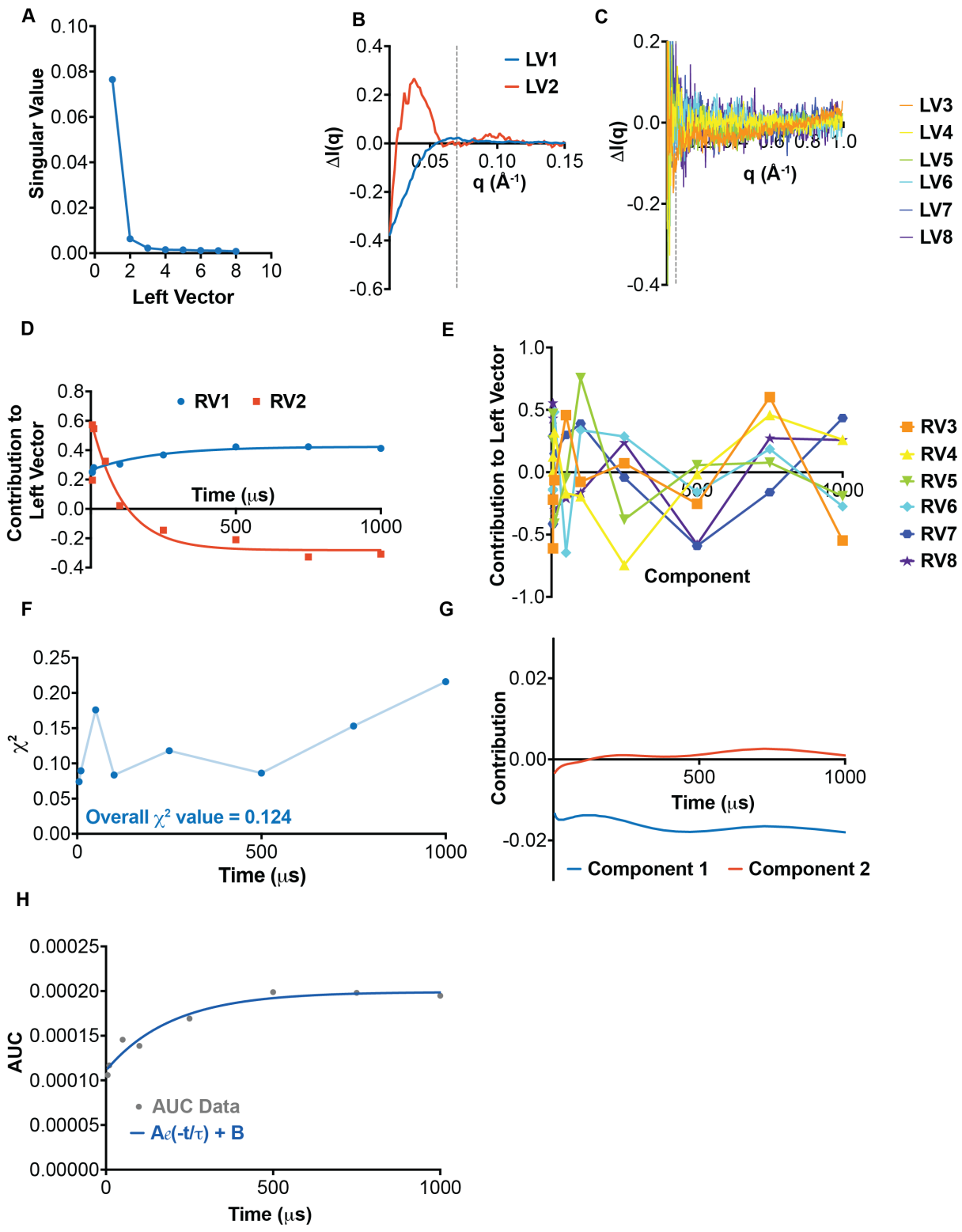

Supplemental Figure 9: Decomposition of CH848 Env SOSIP TR, T-Jump SAXS Difference Profiles. (A) The singular values of SVD on CH848 Env SOSIP TR, T-Jump difference profiles

plotted as a function of the extracted SVD vector. **(B)** Singular value decomposition left vectors 1 (*LV1, blue*) and 2 (*LV2, red*) for CH848 SOSIP Env. Dashed grey line at q=0.07Å^{-1} indicates the location of the feature peak. **(C)** CH848 Env SOSIP TR, T-Jump SVD left vectors 3-8. **(D)** Single exponential fits to the SVD right vectors 1 (*RV1, blue*) and 2 (*RV2, red*) showing the contribution of LV1 and LV2 at each time delay. **(E)** CH848 Env SOSIP TR, T-Jump SVD right vectors 3-8. **(F)** c^2 values of the REGALS fit to the TR, T-Jump SAXS data. **(G)** The REGALS concentrations extracted for REGALS component 1 (*blue*) and component 1 (*red*). **(H)** Double exponential fit to AUC for CH848 TR, T-Jump SAXS difference curves.

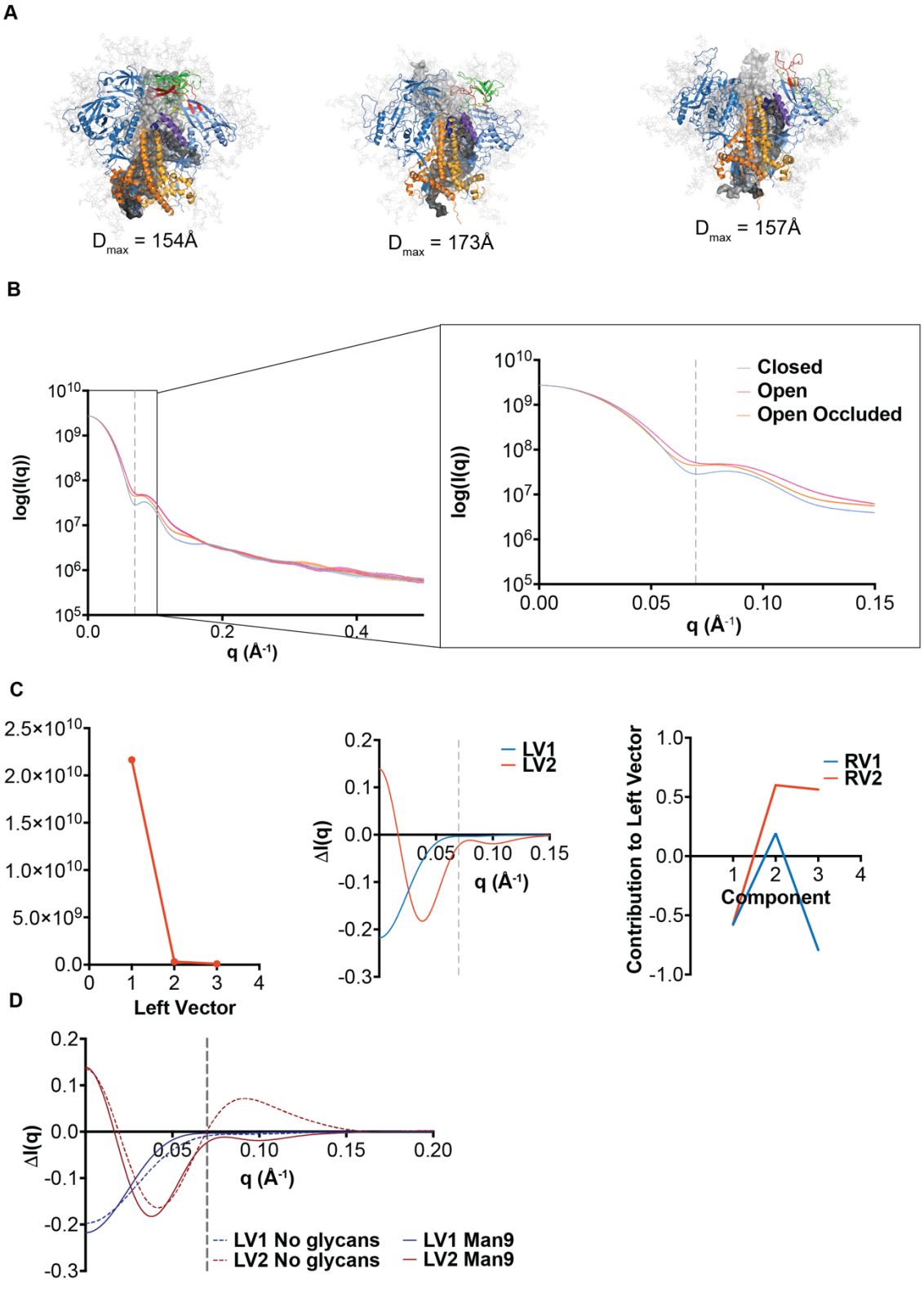

Supplemental Figure 10: CH505 Env SOSIP Model Glycosylated with Mannose-9. (A) All-atom models of CH505 Env SOSIP glycosylated with Man9 in the closed (*left*), Open-Occluded

(*middle*), and Open conformations (*right*). **(B)** The theoretical SAXS scattering profiles showing the scattering intensity in the log scale as a function of the scattering vector in $Å^{-1}$ for Man9 glycosylated 3Closed (*blue*), OpenOccluded (*orange*), and Open (*pink*) CH505 Env SOSIP models. The box shows the region detailed in the inset and the grey dash line depicts the feature peak. The standard errors of the arithmetic mean are shown as shaded regions in the plots. **(C)** The singular values of singular value decomposition (SVD) on CH505 Env SOSIP TR, T-Jump difference profiles plotted as a function of the extracted SVD vector (*left*). SVD left vectors 1 (LV1, *blue*) and 2 (LV2, *red*; *middle*). Dashed grey line at $q=0.07Å^{-1}$ indicates the location of the feature peak. The SVD right vectors 1 (RV1, *blue*) and 2 (RV2, *red*) showing the contribution of LV1 and LV2 at each time delay (*right*). **(D)** SVD first left vectors (LV1, *blue*) and second left vectors (LV2, *red*) for Man9 glycosylated (*solid*) and non-glycosylated (*dashed*) CH505 Env SOSIP models.

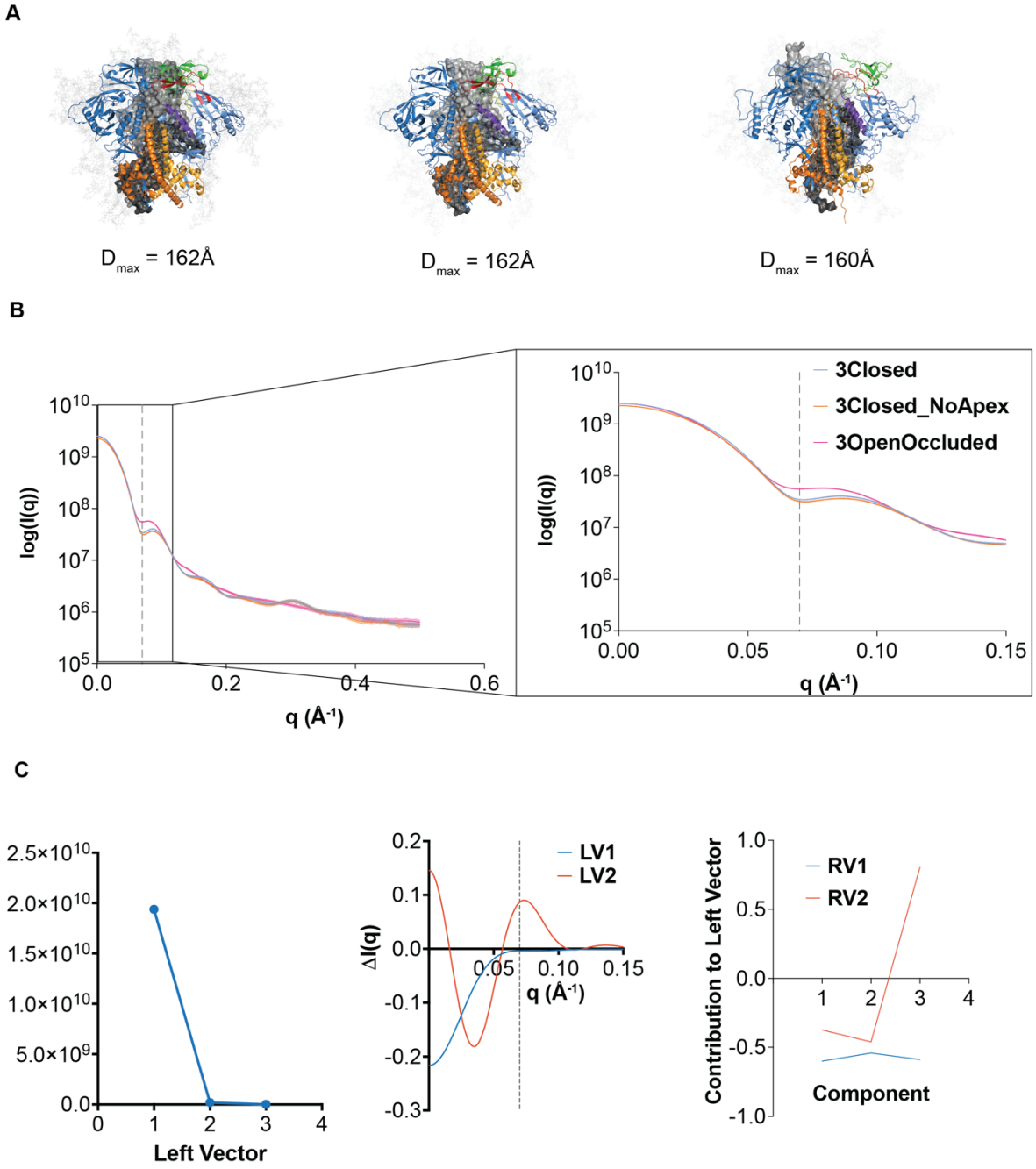

Supplemental Figure 11: CH848 Env SOSIP Model Glycosylated with Mannose-9. (A) All-atom models of CH848 Env SOSIP glycosylated with Man9 in the closed (*left*), Clsoed_NoApex

(*middle*), and Open-Occluded (*right*) conformations. **(B)** The theoretical SAXS scattering profiles showing the scattering intensity in the log scale as a function of the scattering vector in $Å^{-1}$ for Man9 glycosylated 3Closed (*blue*), Closed_NoApex (*orange*), and OpenOccluded (*pink*) CH848 Env SOSIP models. The box shows the region detailed in the inset and the grey dash line depicts the feature peak. The standard errors of the arithmetic mean are shown as shaded regions in the plots. **(C)** The singular values from SVD on CH848 Env SOSIP TR, T-Jump difference profiles plotted as a function of the extracted SVD vector (*left*). SVD left vectors 1 (*LV1, blue*) and 2 (*LV2, red*; *middle*). Dashed grey line at $q=0.07Å^{-1}$ indicates the location of the feature peak. The SVD right vectors 1 (*RV1, blue*) and 2 (*RV2, red*) showing the contribution of LV1 and LV2 at each time delay (*right*).

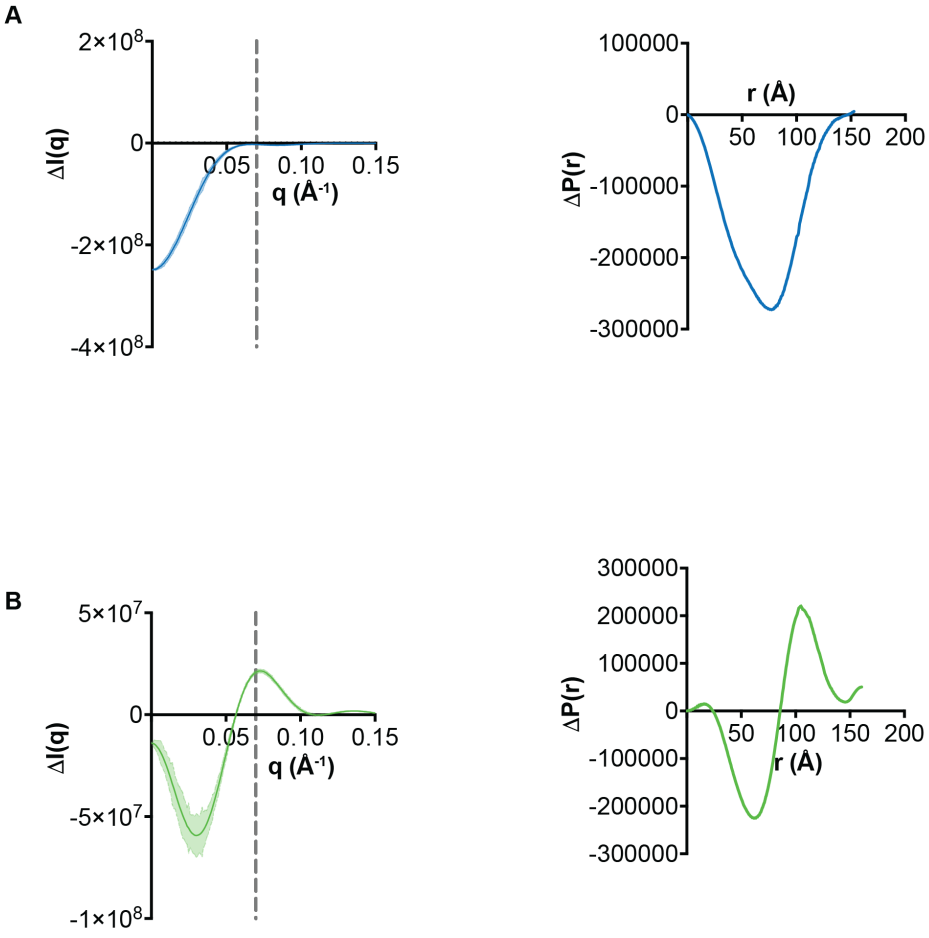

Supplementary Figure 12: CH848 SOSIP Env exhibits same opening transitions as CH505 SOSIP Env. (A) The theoretical difference curve (*left*) and the theoretical pair distance distribution difference curve (*right*) for the release of the Env SOSIP trimer apex contacts. **(B)** The theoretical difference curve (*left*) for and the theoretical pair distance distribution difference curve (*right*) for the closed to open-occluded transition in CH848.

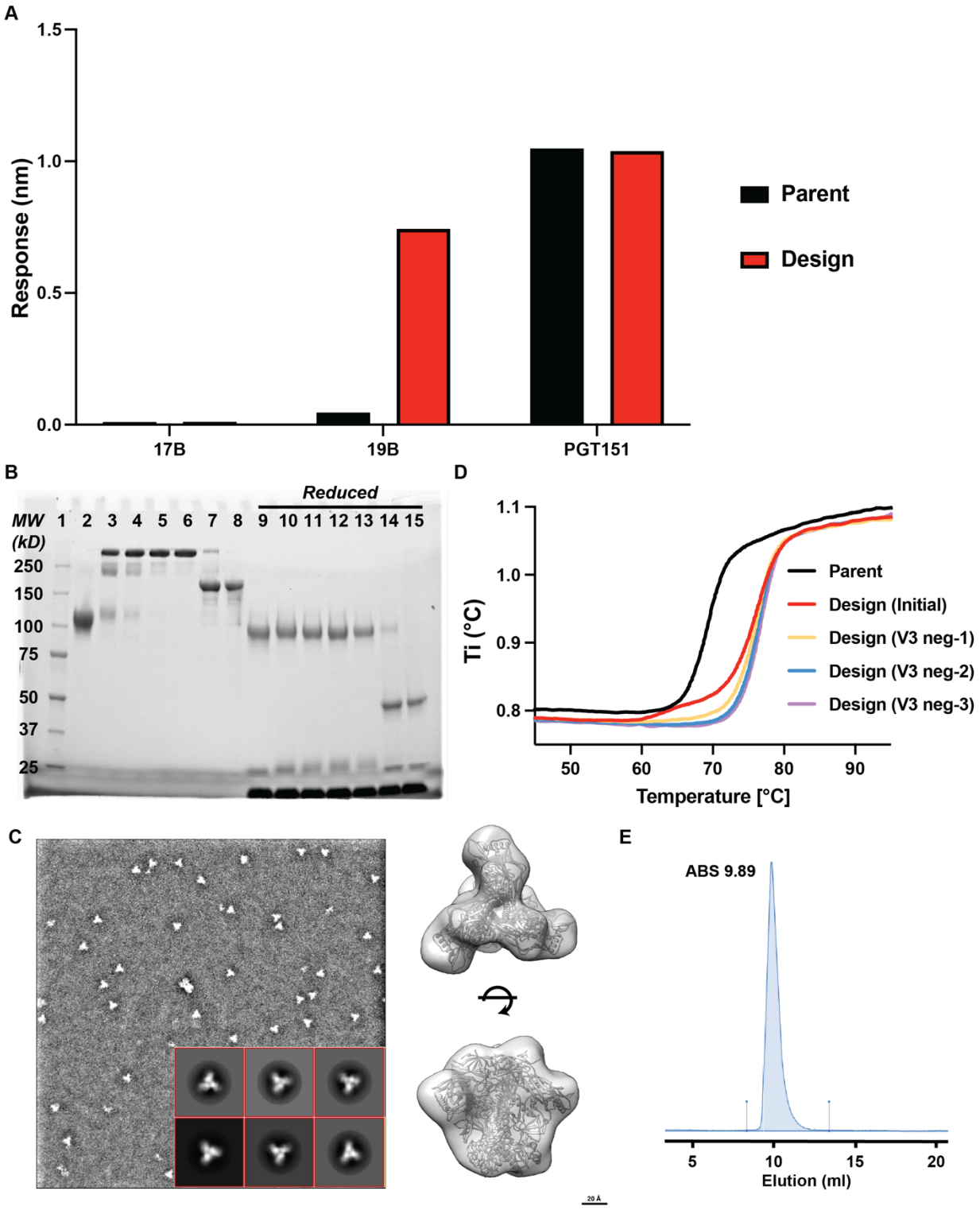

Supplemental Figure 13: CH505 apex staple design. (A) Biolayer interferometry binding responses for 17b, 19b, and PGT151 mAbs interacting with the parent and apex stapled design

Env SOSIPs. **(B)** SDS-PAGE gel. Lanes are as follows: 1- Molecular weight protein marker, 2- Parent SOSIP, 3- PGT151 purified CH505 design prior to V3 interactive 3074 based negative selection, 4-6- Sequential rounds of negative selection, 7 & 8- Eluant from Protein A column post V3 negative selection, 9-15- Reduced samples from 2-8. **(C)** Representative NSEM micrograph, 2D-class averages, and 3D reconstruction. **(D)** Differential scanning fluorescence based thermal melting profiles for the parent CH505 SOSIP and the apex stapled CH505 SOSIP design pre- and post-V3 negative selection iterations. **(E)** Analytical SEC profile for the final round of V3 negative selection.

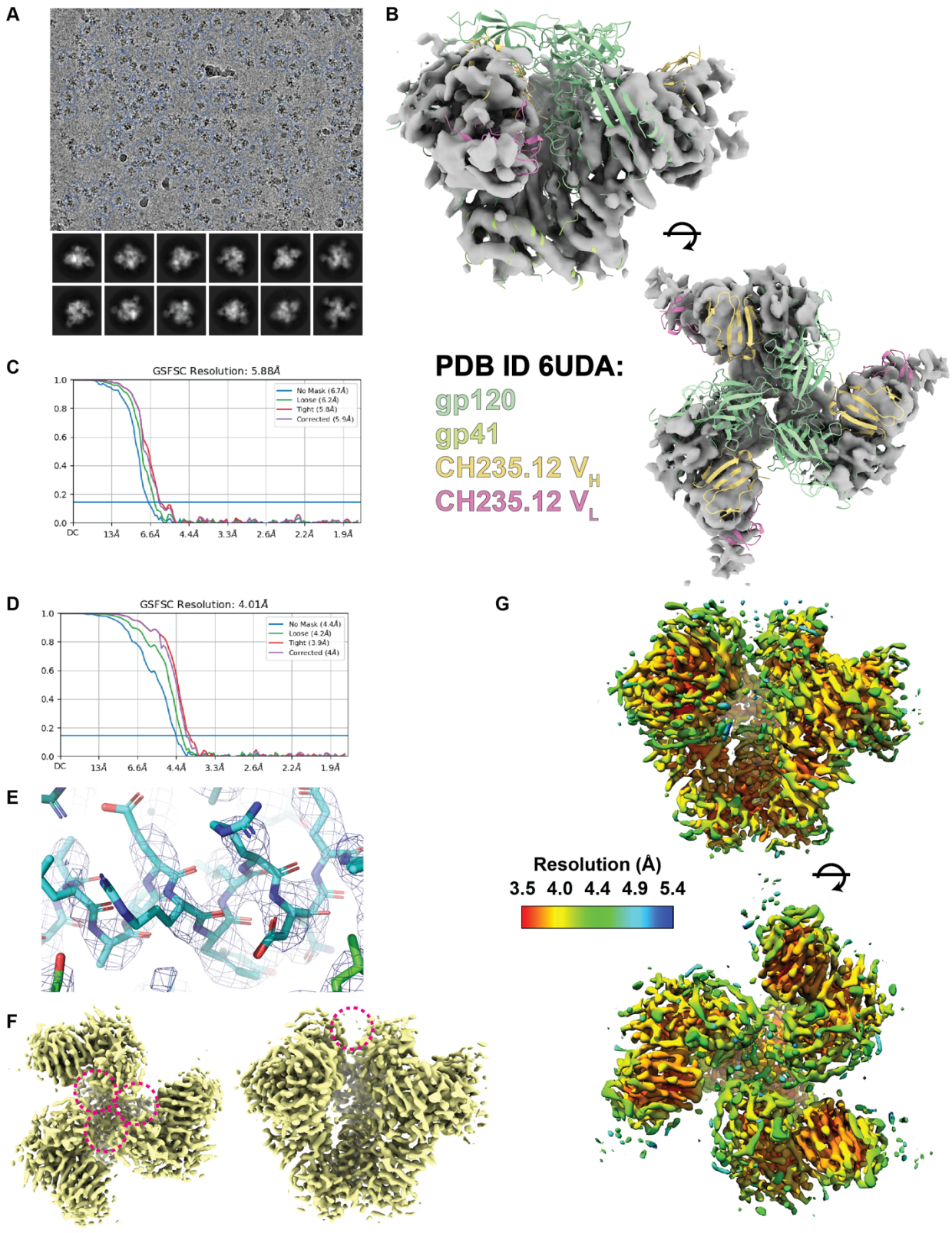

Supplemental Figure: 14 Cryo-EM of CH505 apex staple design. (A) Representative cryo-EM micrograph and 2D-class averages for the apex stapled CH505 design bound to the

CH235.12 Fab. **(B)** Open state map aligned with a closed state CH505 SOSIP model bound to CH235.12 Fab. **(C)** FSC plot for the Open state map. **(D)** FSC plot for the closed state map. **(E)** Representative map-to-model fit for the closed state structure. **(F)** Closed state map highlighting weak density at the trimer apex. **(G)** Local resolution map for the closed state map.

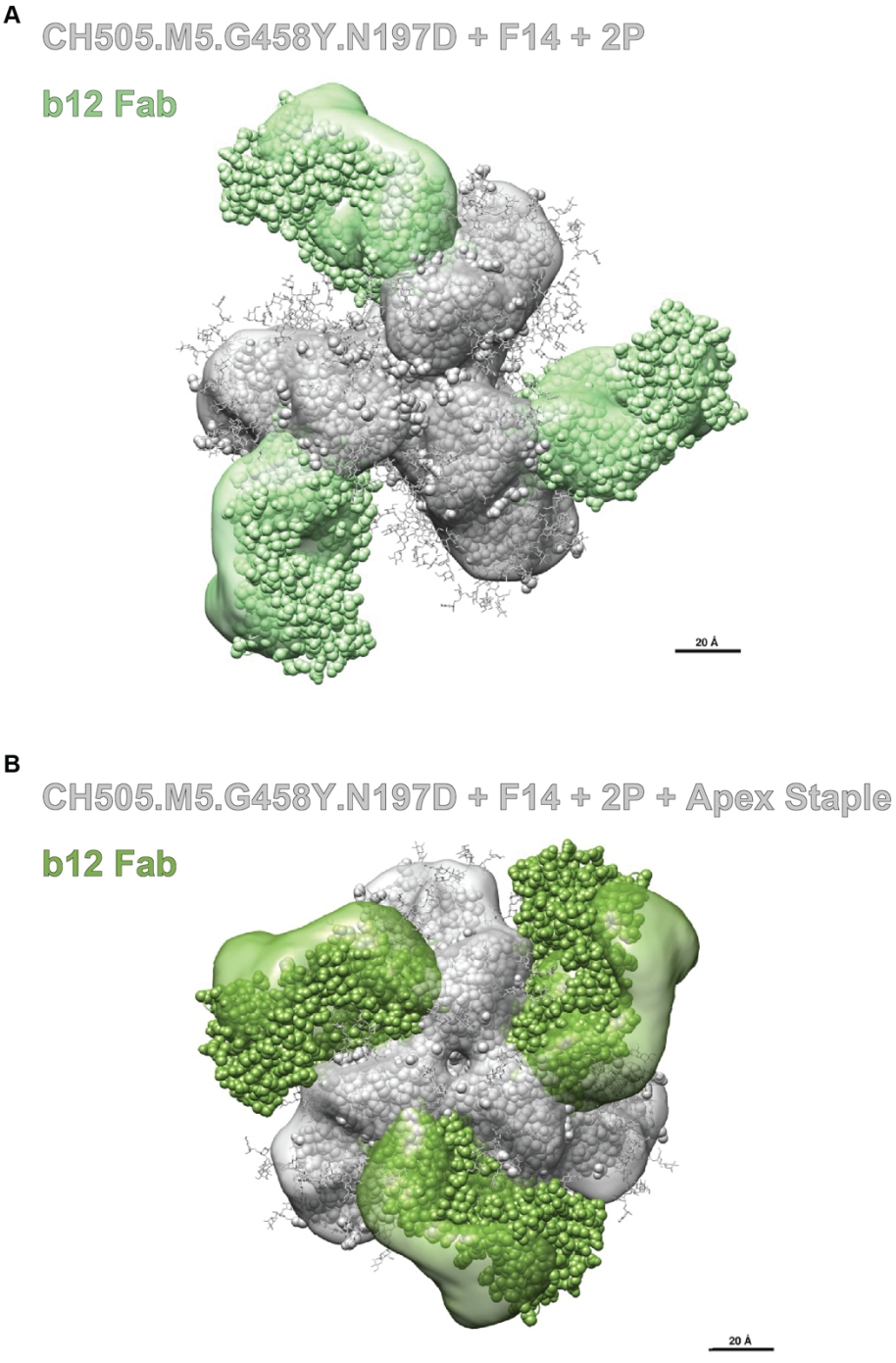

Supplemental Figure 15: NSEM of CH505 apex staple bound to b12. (A) Negative state 3D map and model fit of the non-apex stapled parent SOSIP (grey) bound to the b12 Fab (green)

(**B)** Negative state 3D map and model fit of the apex stapled design SOSIP (grey) bound to the b12 Fab (green)

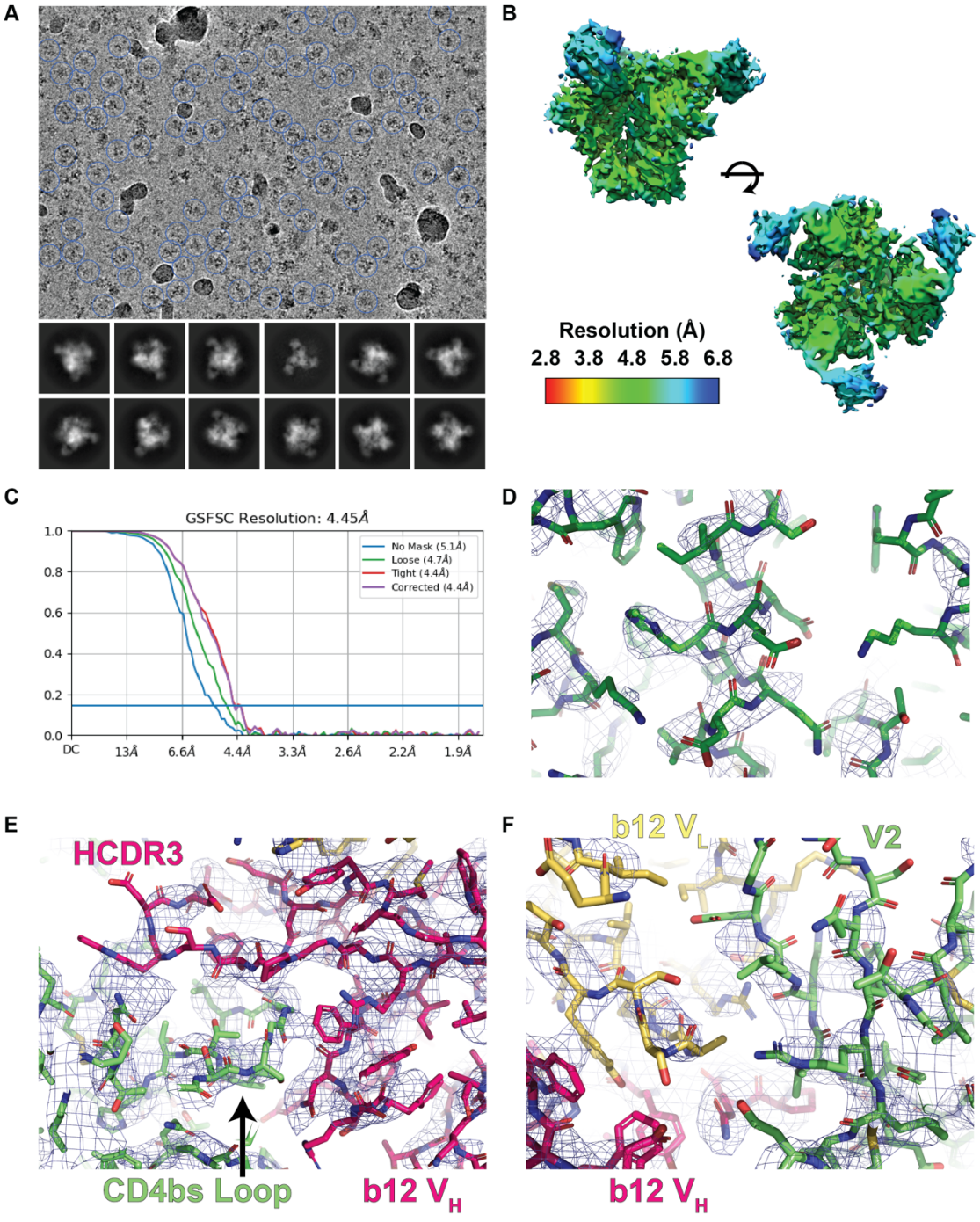

Supplemental Figure 16: Cryo-EM of CH505 apex staple bound to b12. (A) Representative cryo-EM micrograph and 2D-class averages for the apex stapled CH505 design bound to the b12 Fab. **(B)** Local resolution map. **(C)** FSC plot for the b12 bound map. **(D)** Representative map-to-model fit. **(E)** Representative map-to-model fit in the region of the b12 HCDR3 to gp120 CD4bs contact. **(F)** Representative map-to-model fit in the region of the b12 V_L to gp120 V2 loop contact.

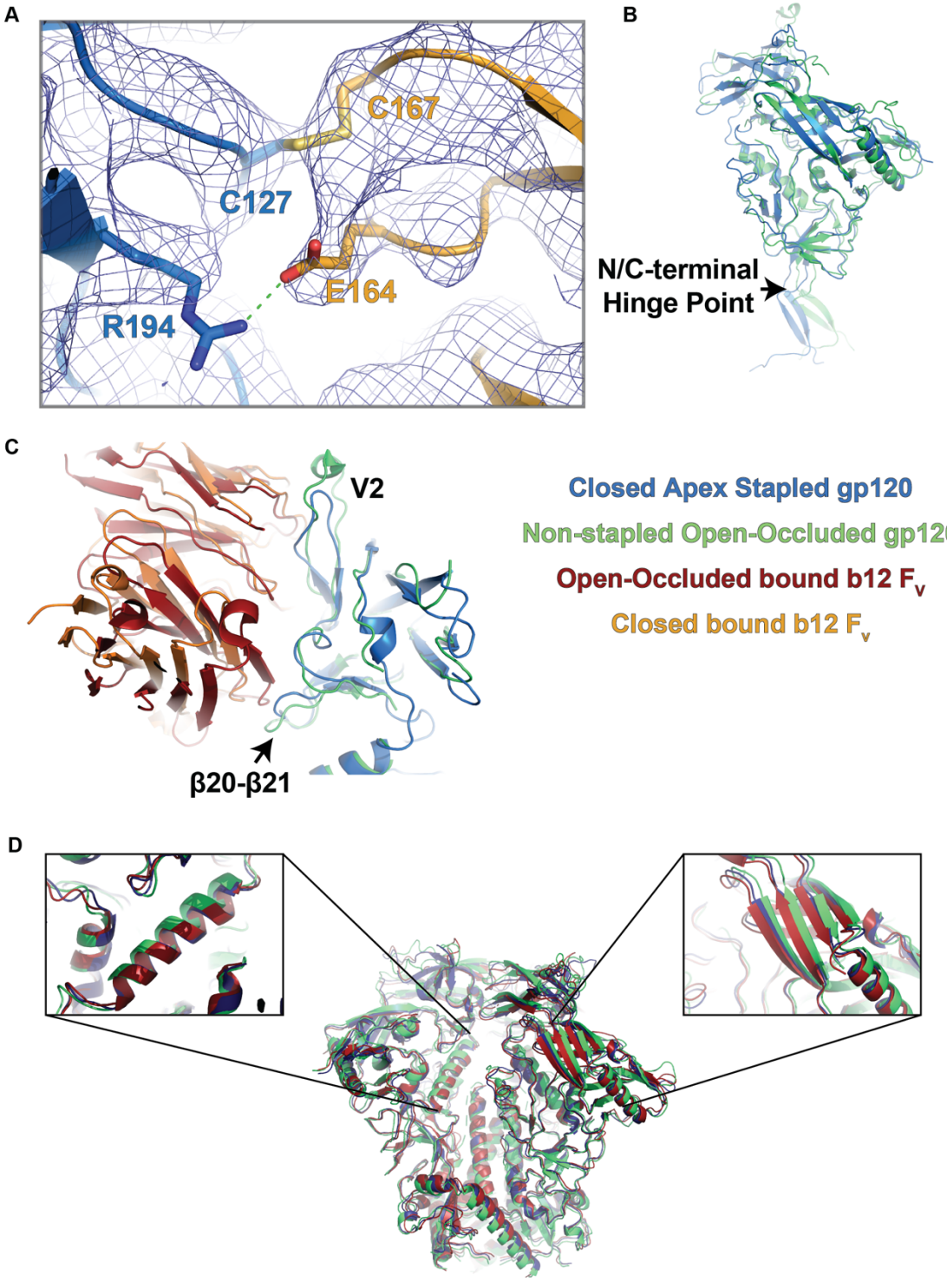

RMSD (Å)	CH505 + CH235.UCA	CH505.AS + CH235.12	CH505.AS + b12
CH505 + CH235.UCA	0.0	1.3	1.9
CH505.AS + CH235.12	1.3	0.0	1.4
CH505.AS + b12	1.9	1.4	0.0

Supplemental Figure 17: Angle of binding for b12 is shifted in the CH505 apex staple design. (A) Map to model fit depicting the introduced inter-protomer apex staple. **(B and C)** Alignment of the b12 bound apex stapled CH505 SOSIP design and B41 isolate gp120 domains highlighting differences and similarities of ***(B)*** gp120 domains ***(C)*** and β20-β21 and V2 loops. **D)** Alignments of the CH505+CH235.UCA (green), CH505+CH235.12 (blue), and CH505+b12 (red).

Static SAXS R_g			
Data Set	**Guinier Rg (Å)**	**P(r) Rg (Å)**	**dmax (Å)**
CH505	53.35 ± 0.12	52.37 ± 0.04	161.31
CH505_W53	53.89 ± 0.19	53.63 ± 0.04	167.13
CH505_W78	51.33 ± 0.16	50.67 ± 0.62	159.82
CH505_W100	52.33 ± 0.23	52.33 ± 0.08	171.98
CH505_4.1	51.23 ± 0.11	50.29 ± 0.14	182.32
BG505	50.31 ± 0.12	48.59 ± 0.18	207.04

Supplemental Table 1: Radius of gyration (R_g) values determined for experimental static SAXS scattering profiles.

Temperature Series Static SAXS R_g						
Data Set	**CH505**			**CH848**		
	Guinier Rg (Å)	**P(r) Rg (Å)**	**dmax (Å)**	**Guinier Rg (Å)**	**P(r) Rg (Å)**	**dmax (Å)**
25°C	45.66 ± 0.58	51.17 ± 0.25	154.68	Not measured	Not measured	Not measured
30°C	Not measured	Not measured	Not measured	55.70 ± 0.24	51.22 ± 0.25	152.80
35°C	45.74 ± 0.58	51.21 ± 0.25	153.60	55.62 ± 0.13	51.22 ± 0.24	152.78
40°C	Not measured	Not measured	Not measured	55.74 ± 0.26	51.24 ± 0. 25	152.83
44°C	45.90 ± 0.57	51.73 ± 0.26	155.72	54.75 ± 0.17	51.01 ± 0.22	151.46
50°C	46.36 ± 0.59	51.35 ± 0.25	155.48	Not measured	Not measured	Not measured

Supplemental Table 2: Radius of gyration (R_g) values determined for experimental temperature series static SAXS scattering profiles.

TR, T-Jump R_g						
Time Delay	**CH505**			**CH848**		
	Guinier Rg (Å)	**P(r) Rg (Å)**	**dmax (Å)**	**Guinier Rg (Å)**	**P(r) Rg (Å)**	**dmax (Å)**
500ns	42.98	50.22	145.66	Not measured	Not measured	Not measured
1.5us	46.14	51.19	154.63	Not measured	Not measured	Not measured
3us	46.1	51.19	154.5	Not measured	Not measured	Not measured
5us	46.12	51.2	154.53	55.15 ± 0.23	51.13 ± 0.24	151.45
10us	42.76	51.07	152.59	55.16 ± 0.22	51.14 ± 0.22	151.36
50us	42.71	51.05	153.46	55.16 ± 0.22	51.16 ± 0.24	151.29
100us	42.74	51.09	152.49	55.15 ± 0.22	51.21 ± 0.23	151.43
250us	Not measured	Not measured	Not measured	54.96 ± 0.23	51.03 ± 0.24	153.05
500us	42.79	51.06	153.24	55.16 ± 0.22	51.14 ± 0.22	150.67
750us	Not measured	Not measured	Not measured	54.98 ± 0.22	51.00 ± 0.23	153.09
1ms	42.79	51.13	153.23	55.17 ± 0.23	51.16 ± 0.25	151.22
10ms	40.79	51.25	153.85	54.94 ± 0.23	51.07 ± 0.29	154.46
100ms	40.77	51.22	154.5	54.94 ± 0.22	51.04 ± 0.26	153.09

Supplemental Table 3: Radius of gyration (R_g) values determined for experimental TR, T-Jump SAXS scattering profiles.

		Kinetic Fits					
Data Set	**Analysis**	**Model**	**a**	**τ_1**	**b**	**τ_2**	**c**
CH505	RV1	Double exponential	-0.064 ± 0.009	7 ± 2 μs	-0.28 ± 0.01	466 ± 63 μs	0.57 ± 0.01
	RV2	Single exponential	1.3 ± 0.2	789 ± 183	-1.0 ± 0.2	N/A	N/A
	AUC	Double exponential	-0.000034 ± 0.000004	7 ± 2 μs	-0.000246 ± 0.000007	502 ± 40	0.000430 ± 0.000008
CH848	RV1	Single exponential	-0.16 ± 0.02	213 ± 69 μs	0.42 ± 0.01	N/A	N/A
	RV2	Single exponential	0.90 ± 0.04	110 ± 15 μs	-0.28 ± 0.03	N/A	N/A
	AUC	Single exponential	-0.000088 ± 0.000008	197 ± 55	0.000199 ± 0.000006	N/A	N/A

Supplemental Table 4: Kinetic fits to TR, T-Jump SAXS data.

Theoretical Rg				
Isolate	**Model**	**Guinier Rg (Å)**	**P(r) Rg (Å)**	**dmax (Å)**
CH505	Closed + Man9	52.11 ± 0.03	51.97 ± 0.04	153.56
	Closed_NoApex + Man9	52.36 ± 0.03	52.19 ± 0.05	153.34
	OpenOccluded + Man9	53.36 ± 0.02	53.32 ± 0.06	161.36
	3Open + Man9	50.85	50.9	156.2
CH848	Closed + Man 9	51.09 ± 0.02	51.02 ± 0.05	152.04
	Closed_NoApex + Man9	50.92 ± 0.02	50.87 ± 0.06	152.77
	OpenOccluded + Man9	52.62 ± 0.03	52.65 ± 0.06	160.67

Supplemental Table 5: Radius of gyration (R_g) values determined for theoretical SAXS scattering profiles